Novel, benign, solid catalysts for the oxidation of hydrocarbons

Paul Ratnasamy, Robert Raja and Darbha Srinivas

References	**This article cites 21 articles** http://rsta.royalsocietypublishing.org/content/363/1829/1001.full.html#ref-list-1
Email alerting service	Receive free email alerts when new articles cite this article - sign up in the box at the top right-hand corner of the article or click **here**

To subscribe to *Phil. Trans. R. Soc. A* go to:

http://rsta.royalsocietypublishing.org/subscriptions

Novel, benign, solid catalysts for the oxidation of hydrocarbons

By Paul Ratnasamy[1], Robert Raja[2] and Darbha Srinivas[1]

[1]*National Chemical Laboratory, Pune 411 008, India*
(prs@ems.ncl.res.in)
[2]*Department of Chemistry, University of Cambridge, Lensfield Road,
Cambridge CB2 1EW, UK*

The catalytic properties of two classes of solid catalysts for the oxidation of hydrocarbons in the liquid phase are discussed: (i) microporous solids, encapsulating transition metal complexes in their cavities and (ii) titanosilicate molecular sieves. Copper acetate dimers encapsulated in molecular sieves Y, MCM-22 and VPI-5 use dioxygen to regioselectively *ortho*-hydroxylate L-tyrosine to L-dopa, phenol to catechol and cresols to the corresponding *o*-dihydroxy and *o*-quinone compounds. Monomeric copper phthalocyanine and salen complexes entrapped in zeolite-Y oxidize methane to methanol, toluene to cresols, naphthalene to naphthols, xylene to xylenols and phenol to diphenols. Trimeric μ_3-oxo-bridged Co/Mn cluster complexes, encapsulated inside Y-zeolite, oxidize *para*-xylene, almost quantitatively, to terephthalic acid. In almost all cases, the intrinsic catalytic activity (turnover frequency) of the metal complex is enhanced very significantly, upon encapsulation in the porous solids. Spectroscopic and electrochemical studies suggest that the geometric distortions of the complex on encapsulation change the electron density at the metal ion site and its redox behaviour, thereby influencing its catalytic activity and selectivity in oxidation reactions.

Titanosilicate molecular sieves can oxidize hydrocarbons using dioxygen when loaded with transition metals like Pd, Au or Ag. The structure of surface Ti ions and the type of oxo-Ti species generated on contact with oxidants depend on several factors including the method of zeolite synthesis, zeolite structure, solvent, temperature and oxidant. Although, similar oxo-Ti species are present on all the titanosilicates, their relative concentrations vary among different structures and determine the product selectivity.

Keywords: solid catalysts; benign catalytic oxidations;
encapsulated metal complexes; titanosilicate molecular sieves

1. Introduction

Many industrial oxidations in the liquid phase are presently carried out with homogeneous catalysts. Such oxidations generate toxic effluents, which require extensive clean-up and catalyst separation procedures. Discovery of environmentally benign, solid catalysts for such oxidations using H_2O_2 or dioxygen as the oxidant, is currently one of the major challenges in heterogeneous catalysis (Thomas *et al.* 2001).

In the present study, we describe two classes of solid catalysts for the liquid phase oxidation of hydrocarbons using dioxygen, as well as H_2O_2, as oxidants. The first class includes microporous solids, encapsulating in their cavities monomeric as well as polymeric transition metal complexes. The ligand environment and molecular confinement (in the case of encapsulated complexes) influence the redox potential at the metal ion, and as a consequence, its catalytic activity and selectivity. The second class consists of titanosilicate molecular sieves. Both these catalysts are rugged and easily separable from the reaction mixtures. Unlike the homogeneous counterparts, the solid catalysts are not easily deactivated during the oxidation reactions and could be recycled (Raja & Ratnasamy 1995, 1997*a,b*; Jacob *et al.* 1998; Raja *et al.* 1999; Chavan *et al.* 2001).

Using EPR and diffuse reflectance UV–visible spectroscopies we had, earlier, identified different types of Ti sites and oxo-Ti species (hydroperoxo-, peroxo- and superoxo-Ti) generated on contact of titanosilicates with oxidants such as H_2O_2, $H_2 + O_2$ and urea-H_2O_2 (Chaudhari *et al.* 2001; Shetti *et al.* 2003, 2004; Srinivas *et al.* 2003). We find that the relative concentrations of these different oxo species influence the activity and product selectivity of titanosilicate molecular sieves in oxidation reactions.

2. Experimental

(*a*) *Materials*

The molecular sieve-encapsulated CuAc, Cu(salen), CuPc and Co/Mn cluster complexes and titanosilicate molecular sieves were prepared as reported by us earlier (Raja & Ratnasamy 1995, 1997*a,b*; Jacob *et al.* 1998; Raja *et al.* 1999; Chaudhari *et al.* 2001; Chavan *et al.* 2001; Shetti *et al.* 2003, 2004; Srinivas *et al.* 2003).

(*b*) *Reaction procedures and product analysis*

(i) *Regioselective* ortho-*hydroxylations*

In a typical hydroxylation reaction (Raja & Ratnasamy 1995), the solid catalyst (CuAc-Y) was added to the substrate in a phosphate buffer (0.05 M, pH 6.5). The contents were stirred at 298 K in the presence of molecular oxygen for 24 h. Periodically, samples were removed, the solid catalyst was separated by centrifugation and the progress of the oxidation was monitored by HPLC (for L-tyrosine) or gas chromatography (for phenol and cresols).

(ii) *Decomposition of H_2O_2 and* tert-*butyl hydroperoxide (*t-*BuOOH)*

In a typical reaction (Jacob *et al.* 1998) 0.025 g of 'neat' or encapsulated Cu(salen) complex was stirred in 5.5 g of H_2O_2 (30% aqueous) or 5 g of *t*-BuOOH at 298 K for 1 h. In H_2O_2 decomposition, after filtration of the catalyst, the product was diluted with water to 250 ml. To 10 ml of this solution, 20 ml dilute H_2SO_4 (1:20) and 20 ml water were added. The solution was then titrated against standard $KMnO_4$. The decomposition of *t*-BuOOH was monitored by standard iodimetry.

(iii) *Oxidation of methane, propane and allyl alcohol*

Oxidation of methane, propane and allyl alcohol were carried out as described earlier (Raja & Ratnasamy 1997*a*,*b*; Raja *et al.* 1999; Shetti *et al.* 2003).

(iv) *Epoxidation of styrene over TS-1 using H_2O_2 as oxidant and hydroquinone as radical scavenger*

In a 100 ml Teflon-lined steel autoclave, 100 mg of TS-1, 10 g of CH_3CN, 8.62 mmol styrene, 17.2 mmol of H_2O_2 (30% aqueous) and hydroquinone (0–0.018 mmol) were taken and the reaction was conducted at 333 K, rotating speed of 30 r.p.m. and for 8 h. The products were analysed by gas chromatography/mass spectrometry.

(v) *Epoxidation of cyclohexene using titanosilicate and horseradish peroxidase*

In a typical reaction 100 mg of titanosilicate (TS-1, Ti-MCM-41, Ti-SBA-15), 0.82 g of cyclohexene, 3.28 g of CH_3CN were taken in a glass flask fitted with a water-cooled condenser and placed in a constant temperature (333 K) oil bath. To it, H_2O_2 (30% aqueous) was added drop-wise over a period of 10 min, and then the reaction was carried out for 4 h. The products were analysed by gas chromatography.

In the reactions with horseradish peroxide (HRP, SRL, India), 82 mg of cyclohexene, 0.128 mmol H_2O_2, 0.5 ml of CH_3CN and 1 ml of 100 µM HRP in phosphate buffer were taken in a glass rector and the reaction was carried out at 298 K for 1.5 h. The product was extracted with 10 ml of diethyl ether (three times) and analysed by gas chromatography.

The characterization of the catalysts has been described in our earlier publications (Raja & Ratnasamy 1995, 1997*a*,*b*; Jacob *et al.* 1998; Raja *et al.* 1999; Chaudhari *et al.* 2001; Chavan *et al.* 2001; Shetti *et al.* 2003, 2004; Srinivas *et al.* 2003).

3. Results and discussion

(*a*) *Zeolite-encapsulated metal complexes*

(i) *Regioselective* ortho-*hydroxylation-tyrosinase mimics*

Copper acetate (CuAc), encapsulated in molecular sieves Y, MCM-22 and VPI-5 regioselectively *ortho*-hydroxylates ʟ-tyrosine to ʟ-dopa and subsequently to dopaquinone in phosphate buffer (pH 6.5) at 298 K using atmospheric dioxygen as oxidant (scheme 1; table 1). The pH specificity as well as the temperature dependence of the reaction suggests that the CuAc complex is active only when it is present as a dimer (Raja & Ratnasamy 1995). When the dimeric structure is absent (lower pH or higher temperatures) the complex is inactive.

The molecular sieve-based catalysts showed a high substrate and regio-specificity (Raja & Ratnasamy 1995). Only mono and *o*-dihydroxy aromatic compounds (like phenol, catechol and cresols) underwent oxidation, though at varying rates (table 1). Aromatic substrates without a phenolic OH group were not
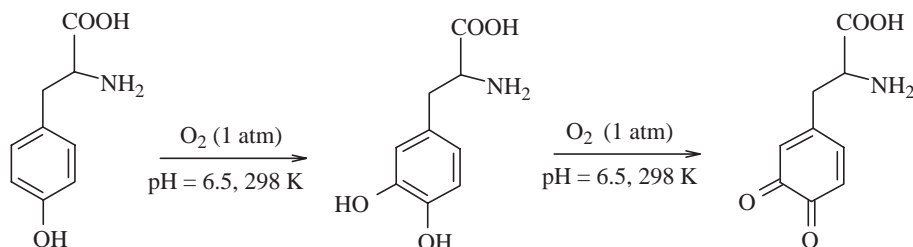
Scheme 1.

Table 1. *Catalytic activity (TON) in the oxidation of* L*-tyrosine, phenol,* o*-cresol and* m*-cresol*
(Reaction conditions: catalyst, 0.02–0.04 g; phosphate buffer, 0.05 M, pH 6.5; molecular oxygen, 1 atm; substrate, L-tyrosine (2 dM), phenol (8 wt%), o- and m-cresols (15 wt% in phosphate buffer); temperature, 298 K; reaction time, 24 h.)

catalyst	TON[a]			
	L-tyrosine	phenol	o-cresol	m-cresol
CuAc-'neat'	2.9	3.8	7.2	5.2
CuAc-HY	15.2	22.1	56.4	50.9
CuAc-MCM-22	27.6	35.6	71.5	55.8
CuAc-VPI-5	10.5	20.2	45.7	33.8

[a]Turnover number (TON), moles of substrate converted per mole of Cu.

oxidized. Oxidation of phenol, for example, yielded only catechol/o-benzoquinone; the *para*-isomers, hydroquinone/p-benzoquinone were not observed. In all these hydroxylation reactions the encapsulated CuAc dimers exhibited higher catalytic activity than the corresponding 'neat' complexes (table 1).

EPR confirmed the presence of CuAc dimers in the supercages of zeolite-Y (Chavan *et al.* 2000b). The spins on the two Cu(II) centres of the dimer (3d^9, $S=1/2$) were coupled anti-ferromagnetically resulting in a groundstate singlet ($S=0$) and a low-lying excited-state triplet ($S=1$). At ambient temperatures, the triplet state was populated and the complex exhibited paramagnetism (1.4 B.M.). As the temperature is lowered (from ambient temperature to 77 K), the excited triplet levels were depopulated and the dimer signal intensity decreased. Variable temperature measurements enabled the estimation of intramolecular Cu–Cu exchange coupling constant (J) and Cu–Cu distance (r) in the dimer (Chavan *et al.* 2000b). The exchange interaction (J) between the Cu(II) ions in the dimer increased upon encapsulation from 259 to 310 cm^{-1}; the Cu–Cu distance (r) decreased for the encapsulated CuAc from 2.64 to 2.40 Å. The value of 2.64 Å (from EPR spectroscopy) for 'neat' CuAc matches well with the reported value from the single crystal X-ray diffraction study (2.61 Å; De Meester *et al.* 1973).

The short Cu–Cu distance and the consequent greater, lateral overlap of the Cu orbitals would facilitate the transfer of electron density from the phenolate ligand to the antibonding LUMO of the complex, thereby weakening the copper peroxide, O–O bond formed by the coordination of O$_2$ to the copper complex. Weakening of the O–O bond would, in turn, make it easier for the cleavage and

the transfer of one of the two oxygens of the peroxide ligand to the position *ortho* to the phenolate bond. Under the reaction conditions (pH 6.5), the phenols exist in the phenolate form.

(ii) *Decomposition of peroxides: catalase activity*

Copper salen complexes encapsulated inside the supercages of zeolite-Y exhibit catalase activity with rates of decomposition of H_2O_2 or *t*-butyl hydroperoxide (10^5) approaching those of natural catalase enzymes (Jacob *et al.* 1998). Substitution of the aromatic hydrogen atoms of the salen ligand by electron withdrawing groups like Cl, Br and NO_2 enhances the catalytic activity. The encapsulated complexes exhibit higher turnover frequencies (TOF) by several orders of magnitude than the corresponding 'neat' complexes (Jacob *et al.* 1998). Similar enhancements in the activity were observed also for the oxidation of styrene and aerobic oxidation of *para*-xylene with these complexes (Jacob *et al.* 1998).

'Neat' Cu(salen) in the solid state is dimeric with a tetragonally elongated square pyramidal geometry around Cu (Deshpande *et al.* 1999). In the dissolved state and in non-coordinating solvents, the complex exists as monomers with square planar geometry. In the encapsulated complex, Cu(salen) is present as monomers (as in the dissolved state) in the supercages of zeolite-Y and possesses tetrahedrally distorted-square planar geometry (Deshpande *et al.* 1999). The orbital coefficients and ground state wave functions (estimated from the spectral parameters) are modified considerably for the encapsulated complexes. The in-plane covalency of the Cu–ligand bond is also increased. Electron density at Cu is depleted by substitution of the aromatic ring H atoms by electron withdrawing groups like Cl or by encapsulation of the complex in the zeolite supercages (Deshpande *et al.* 1999). This depletion of electron density at copper facilitates the attack of incoming nucleophiles like hydroperoxide and *t*-butyl hydroperxoide anions (Deshpande *et al.* 1999). Electrochemical studies confirm that the Cu(II)/Cu(I) reduction potential increases upon encapsulation of the Cu(salen) complex (Jacob *et al.* 1998). The observed changes in the molecular electronic structure and consequent redox properties of the complexes upon encapsulation are, perhaps, responsible for the enhancement in the catalytic activity of the metal salen complexes.

(iii) *C–H bond activation: oxyfunctionalization of alkanes and aromatics*

Metal phthalocyanines (MPc, M = Fe, Co or Cu) encapsulated in zeolites-X, -Y and -L catalyse the direct oxidation of methane (Raja & Ratnasamy 1997*a*) to a mixture of methanol and formaldehyde, and propane (Raja *et al.* 1999) to a mixture of isopropanol and acetone, both at ambient conditions using O_2/t-BuOOH as oxidant (table 2). MPc complexes with electron withdrawing substituents (like Cl and NO_2) exhibit higher activity than the unsubstituted MPc complexes. The intrinsic catalytic activity of the complexes was enhanced by more than two orders of magnitude when the complexes were encapsulated (table 2). Even though methane could be oxidized over these catalysts using O_2 alone, the conversion levels were below 1% and only CO_2 was produced. On the other hand, *t*-BuOOH readily oxidizes methane to methanol and formaldehyde, even in the complete absence of molecular oxygen. At low concentrations of *t*-BuOOH, methanol was the major

Table 2. *Oxidation of methane and propane over MPc complexes*

(Reaction conditions (oxidation of methane): methane, 50 psi; air, 100 psi; CH_3CN, 99.5 g; catalyst, 0.75 g; TBHP, 0.5 g; values in the parentheses refer to the metal content in per cent weight. Reaction conditions (oxidation of propane): propane, 50 psi; air, 200 psi; TBHP, 0.5 g; CH_3CN, 99.5 g; temperature, 298 K; reaction time, 10 h. TON and selectivity values are reproducible to about 10%.)

catalyst[a]	conc. (mol%)	TON[b]	products (mol%): oxidation of methane			
			CH_3OH	HCHO	HCOOH	CO_2
CuPc	0.4	0.09	—	20	—	80
$CuCl_{16}Pc$	4.8	0.72	40.2	47.5	7.2	5.1
$FeCl_{16}Pc$	5.3	0.90	41.2	42.0	8.3	8.5
$CuCl_{16}Pc$-X (0.28)	4.2	48.5	51.5	41.7	4.1	2.7
$FeCl_{16}Pc$-X (0.16)	4.9	107.2	52.6	42.3	3.2	1.9
			products (mol%): oxidation of propane			
			isopropanol	acetone	propylene	CO_2
$CuCl_{16}Pc$	5.0	4.2	63.2	30.5	—	6.3
$FeCl_{16}Pc$	4.8	4.1	42.5	39.7	—	17.8
$CuCl_{16}Pc$-X (0.28)	17.6	316	48.2	37.6	9.2	5.0
$FeCl_{16}Pc$-X (0.16)	13.5	371	39.9	37.8	9.0	13.3

[a]Values in the parentheses refer to the metal content in per cent weight.
[b]Turnover number (TON), moles of substrate converted per mole of Cu.

product. The formation of formic acid and CO_2 increased with increasing concentrations of *t*-BuOOH. When both O_2 and *t*-BuOOH were present there was a synergistic enhancement of methane conversion (Raja & Ratnasamy 1997*a*,*b*). The encapsulated MPc complexes exhibited enhanced catalytic activities also in the oxidation of toluene to cresols, naphthalene to naphthols, xylene to xylenols and phenol to diphenols (Raja & Ratnasamy 1997*a*,*b*).

IR, diffuse reflectance UV–visible and EPR spectroscopic characterizations revealed that CuPc molecules undergo distortion from a planar (D_{4h}) to a puckered (C_{2v}) geometry when they are encapsulated in zeolites (Seelan *et al.* 2000; Ray & Vasudevan 2003). 'Neat' CoPc possesses a centre of inversion (D_{4h}). As a consequence, owing to the mutual exclusion principle, the IR-active vibrational modes are absent in the Raman spectra and *vice versa* in the spectra of 'neat' CoPc complexes (see fig. 5 in Ray & Vasudevan 2003). For the encapsulated complexes, on the contrary, the presence of Raman-active modes in the IR spectra and *vice versa* implies a loss of the centre of inversion in the CoPc molecule indicating a geometric distortion of the complex on encapsulation (Ray & Vasudevan 2003).

Terephthalic acid, a major commodity chemical, is manufactured by the oxidation of *p*-xylene in acetic acid with cobalt and manganese acetates as catalysts and bromide promoters. Such homogeneous metal catalysts generate toxic effluents, which require extensive clean-up and catalyst separation. We had earlier found (Chavan *et al.* 2000*a*), using electronic and EPR spectroscopies that during the *p*-xylene oxidation, heteronuclear μ_3-oxo-bridged Co/Mn cluster complexes

$[CoMn_2(\mu_3\text{-}O; CH_3COO)_6(pyridine)_3]^n$ are the active catalyst species that oxidize *p*-xylene to *p*-toluic acid and further to terephthalic acid. On encapsulation of these cluster complexes inside the super cages of zeolite-Y, the resulting catalyst is an efficient, environmentally benign catalyst for *p*-xylene oxidation (Chavan *et al.* 2001).

(*b*) *Titanosilicate molecular sieves*

Three types of oxo-Ti species, viz. hydroperoxo-, peroxo- and superoxo-Ti, are generated on titanosilicates contacted with H_2O_2 (Notari 1996; Ratnasmy *et al.* 2004). These oxo-Ti species could be identified by DRUV-visible spectroscopy (figure 1, right panel). Only, the superoxo-Ti could be detected by EPR spectroscopy (figure 1, left panel). EPR reveals the presence of three types (A–C) of superoxo-Ti species on TS-1 (Chaudhari *et al.* 2001; Shetti *et al.* 2003, 2004; Srinivas *et al.* 2003). A and B are more abundant than C. These species are present also on Ti-beta and amorphous TiO_2–SiO_2, but in different relative concentrations. Ti-MCM-41 and Ti-SBA-15 generate, predominantly, the B-type species (figure 1, left panel). The concentration of A-type species increases in the following order: amorphous TiO_2–SiO_2 < Ti-beta < TS-1. The B-type species increases in the order: TS-1 < Ti-beta < amorphous TiO_2–SiO_2 < Ti-SBA-15, Ti-MCM-41. Temperature, solvent and oxidant (aqueous H_2O_2, urea–H_2O_2 or (H_2+O_2) mixture) markedly influence the type of oxo-Ti species generated (Srinivas *et al.* 2003). TS-1 prepared from the fluoride medium contains predominantly the B rather than the A-type oxo-Ti species. A comparison of our EPR results with the EXAFS data (Gleeson *et al.* 2000; Thomas & Sankar 2001) suggest that, while the A-type species probably originate from tetrapodally-coordinated Ti sites $(Ti(OSi)_4)$, the B-type originate from the tripodally-coordinated Ti sites $(Ti(OSi)_3(OH))$ and the C-type from a defect site like $Ti(OSi)_3(OH)(OH_2)_2$. EPR spectroscopy provided evidence, for the first time, for the *in situ* generation of such oxo-Ti species over Pd impregnated TS-1 (Pd–TS-1) in the reactions using (H_2+O_2) instead of H_2O_2 (Shetti *et al.* 2003). Pd enhanced the reducibility of Ti and promotes formation of these oxo species at lower temperatures (approximately 323 K). In the absence of Pd, Ti reduction in TS-1 occurs at 823 K. The concentration of the A-type oxo-Ti species is higher than the B and C-types on Pd–TS-1 in the presence of a (H_2+O_2) mixture. It is interesting to note that the epoxide selectivity in the oxidation of allyl alcohol over Pd–TS-1 is higher with (H_2+O_2) than aqueous H_2O_2 (table 3; Shetti *et al.* 2003).

On contact with H_2O_2, TS-1 shows an asymmetric, broad, charge transfer band in the region 300–500 nm (figure 1, right panel). This could be deconvoluted into two bands (I and II) corresponding to superoxo-Ti and hydroperoxo/peroxo-Ti species, respectively. The position and relative intensities of these bands are different in $(TS\text{-}1+H_2O_2)$ and $(TS\text{-}1+urea–H_2O_2)$ systems and in Pd-containing samples. The relative intensity ratio of hydroperoxo- to superoxo-Ti ([II]/[I]) decreases in the following order: $(Pd–TS\text{-}1+H_2O_2)$ (0.73) > TS-1 + H_2O_2 (0.68) > $(TS\text{-}1+urea–H_2O_2)$ (0.43) (figure 1, right panel). In (Ti-MCM-41 + H_2O_2), these bands overlap with the characteristic bands of Ti-MCM-41. Magnetic susceptibility measurements also confirmed the presence of these oxo-Ti species (Srinivas *et al.* 2003).
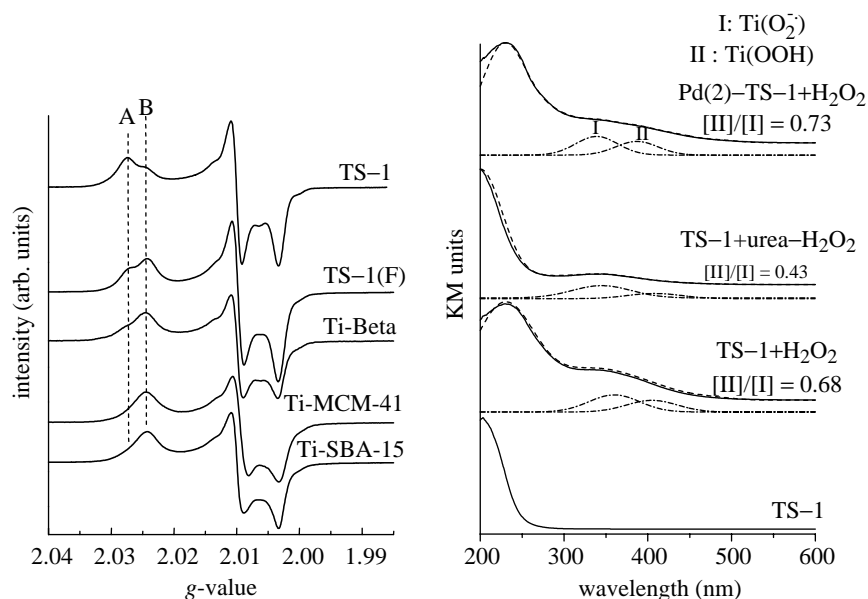
Figure 1. Left: EPR spectra (at 80 K) of titanosilicates interacted with aqueous H_2O_2; g_z signal corresponding to superoxo-Ti species A and B are indicated. TS-1 (F) is TS-1 sample synthesized from fluoride medium. Right: DRUV–visible spectra of TS-1, TS-1+H_2O_2, TS-1+urea–H_2O_2 and Pd(2)-TS-1+H_2O_2. Bands due to superoxo (I) and hydroperoxo (II)-Ti species are marked. Experimental (solid lines), simulated (dashed line) and deconvoluted oxo-titanium bands (dash-dotted line).

Table 3. *Catalytic activity in the epoxidation of allyl alcohol over TS-1 and Pd(n)–TS-1 catalysts* (Reaction medium: catalyst (100 mg)+allyl alcohol (0.5 g)+acetone (10 g)+H_2O_2 (50%, 0.9 ml); temperature, 333 K; run time, 8 h.)

catalyst[a]	oxidant	TOF[b]	H_2O_2 efficiency (%)	conversion (wt%)	epoxide selectivity (wt%)
TS-1	H_2O_2	15.3	42.8	77.0	96.1
Pd(0.5)–TS-1	H_2O_2	12.3	34.2	61.5	95.6
Pd(2)–TS-1	H_2O_2	10.5	28.8	51.7	90.4
Pd(3.5)–TS-1	H_2O_2	7.6	20.7	37.1	82.8
Pd(4.5)–TS-1	H_2O_2	6.2	16.7	30.0	74.0
Pd(2)–TS-1	H_2+O_2	2.1	—	10.5	99.0

[a]Values in parentheses indicate the loading of Pd in wt%.
[b]Turnover frequency (TOF), moles of allyl alcohol converted per mole of Ti per hour.

Controlled EPR experiments on TS-1+H_2O_2+alkene (allyl alcohol or styrene) at 333 K revealed that the superoxo-Ti species are consumed during the reaction. In the absence of alkene, the intensity of type-A species in TS-1 was more than that of type-B (figure 2, left panel). On adding alkene, the concentration of the type-A species decreased faster than that of type-B,
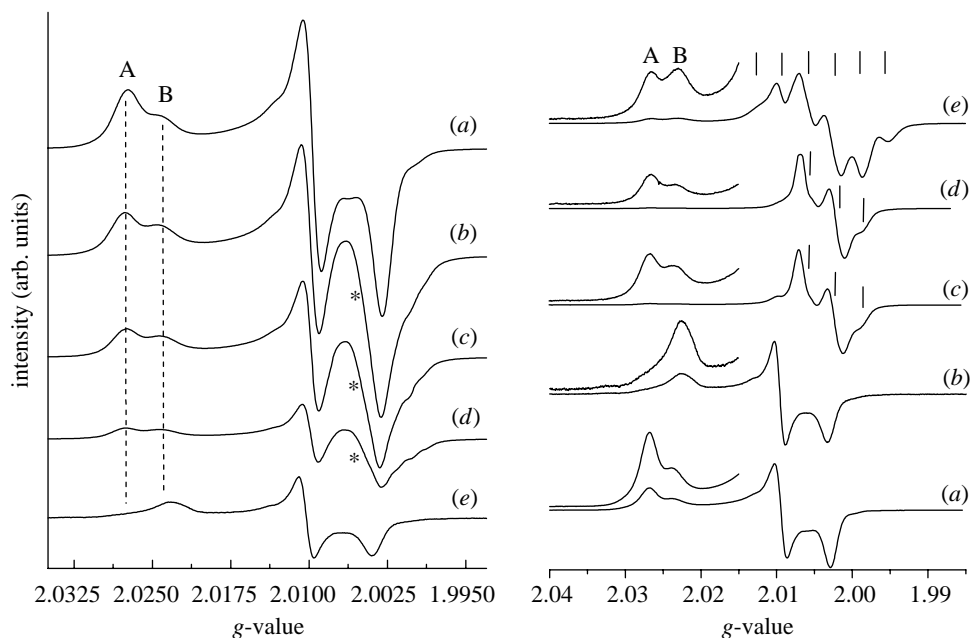
Figure 2. Left: EPR spectra at 90 K. TS-1+H_2O_2+styrene: reaction temp. 333 K and reaction time: (*a*) 0 min, (*b*) 5 min, (*c*) 10 min and (*d*) 20 min. (*e*) TS-1+H_2O_2+allyl alcohol (25 min). Asterisk denotes signals owing to a styrene-based radical formed during the reaction. Right: EPR spectra at 180 K of TS-1+H_2O_2 (*a*) with no substrate, (*b*) with allyl alcohol, (*c*) with phenol, (*d*) with benzene (*e*) with toluene. Signals indicated by vertical lines are owing to substrate-based radicals formed during the oxidation reaction.

indicating the faster consumption of the former. At the end of 25 min, only the B-type species remained (Shetti *et al.* 2003). With styrene as substrate, organic radicals are formed during the reaction. Such radicals were not observed in the reactions with allyl alcohol (figure 2, left panel).

When the TS-1+H_2O_2 slurry was contacted with aromatics such as toluene, benzene or phenol, the colour of the solution changed initially to orange and then to dark blackish-green (Srinivas *et al.* 2003). In the case of phenol and benzene, species B was consumed faster than A. In the case of toluene oxidation, the intensity of both A and B are altered on addition of the substrate.

The catalytic activities of hydroperoxo/peroxo- and superoxo-Ti species in alkene (styrene and cyclohexene) oxidations were investigated by carrying out the experiments with radical scavengers, for example, hydroquinone (HQ). Hydroquinone scavenges the superoxo-Ti species and does not allow it to participate in the catalytic oxidations. In the reaction of styrene, with increasing HQ concentration, the selectivity for styrene oxide increased and benzaldehyde decreased (table 4). This is clear evidence that hydroperoxo-Ti is involved in epoxide formation while superoxo-Ti is involved in non-selective products (e.g. benzaldehyde) formation. Catalytic activity (styrene conversion) decreased with increasing HQ concentration (table 4), since, part of the oxo-Ti species (superoxo-Ti) was scavenged and not used in the epoxidation reaction.

Table 4. *Influence of hydroquinone (HQ) on styrene epoxidation activity*

(Reaction conditions: catalyst (TS-1), 100 mg; styrene, 8.63 mmol, H_2O_2 (30% aq.), 17.2 mmol; solvent (CH_3CN), 10 g; temperature, 333 K; time, 8 h.)

HQ mmol	styrene conv. %	styrene oxide	phenylacetal-dehyde	benzaldehyde	benzoic acid
0	16.4	37.8	12.2	49.3	0.7
0.009	11.5	45.5	12.9	39.8	1.8
0.018	7.9	59.0	12.8	27.2	1.0

Table 5. *Cyclohexene oxidation over titanosilicates and enzymes*

(For reaction conditions see §2*b*(v).)

catalyst	cyclohexene conv. %	TOF (h^{-1})	product selectivity (%)			
			epoxide	-diol	epoxide+diol	allylic products
TS-1	18.6	10	55.6	28.7	84.3	15.7
Ti-MCM-41	34.2	17	12.9	60.3	73.2	26.8
Ti-SBA-15	52.5	25	12.0	62.0	74.1	26.0
Cyt.P450[a]	89.0	1200	85.0	0	85.0	15.0
HRP	66.9	893	64.3	0	64.2	35.8

[a]Data taken from Farinas *et al.* (2004).

Cyclohexene oxidation over different titanosilicates with H_2O_2 as oxidant revealed that the (epoxide+diol) selectivity is more on TS-1 containing tetrapodal Ti sites than on Ti-MCM-41 and Ti-SBA-15 containing the tripodal Ti sites (table 5). It is interesting to note that the selectivity pattern (epoxide+diol, 85% and allylic products, 15%) of TS-1 is similar to that of the monoxygenase enzyme cytochrome P450 (Cyt. P450; Farinas *et al.* 2004). The selectivity patterns (epoxide+diol, 74%; allylic products, 26%) of Ti-SBA-15 and Ti-MCM-41 resemble that of horseradish peroxidase (HRP). It may be noted that the specific catalytic activity over metalloenzymes is two orders of magnitude higher than that over titanosilicates (table 5). Our studies reveal that even though similar oxo species are formed over all the titanosilicates in the presence of either H_2O_2 or H_2+O_2 or urea–H_2O_2, their relative concentration determines the catalytic activity and especially selectivity.

4. Conclusions

The catalytic properties of two classes of solid catalysts, viz. (i) zeolite-encapsulated dimeric copper acetate, monomeric copper salen and phthalocyaine and trimeric (μ_3-oxo)-bridged Co/Mn cluster complexes and (ii) titanosilicate molecular sieves for the oxidation of hydrocarbons are discussed. The intrinsic activity (turnover frequency) of the metal complexes is enhanced upon

encapsulation in the zeolite cavities. Ligand environment and geometric distortions in the encapsulated state markedly affect the electron density at the site of metal ion and its redox properties. As a consequence, catalytic activity and product selectivities can be controlled by a proper choice of the ligands around the metal ion and the cavity wherein the metal complexes are encapsulated.

The chemoselectivity of titanosilicates is influenced by several factors including the method of preparation, zeolite structure, solvent, temperature and oxidant. Spectroscopic studies have identified different types of Ti species (tetrapodal $Ti(OSi)_4$, tripodal $Ti(OSi)_3(OH)$ and other defect Ti sites) on these silicate structures. These Ti have different reduction potentials. On contact with H_2O_2 or (H_2+O_2) or urea–H_2O_2, different types oxo-Ti species, viz. hydroperoxo-, peroxo- and superoxo-Ti, are generated on titanosilicates. Their relative concentrations influence the catalytic activity and product selectivity. The solid catalysts described in this paper are environmentally benign in liquid phase oxidations.

References

Chaudhari, K., Srinivas, D. & Ratnasamy, P. 2001 Reactive oxygen species in titanosilicates TS-1 and TiMCM-41: an *in situ* EPR spectroscopic study. *J. Catal.* **203**, 25–32.

Chavan, S. A., Halligudi, S. B., Srinivas, D. & Ratnasamy, P. 2000*a* Formation and role of cobalt and manganese cluster complexes in the oxidation of *p*-xylene. *J. Mol. Catal. A* **161**, 49–64.

Chavan, S., Srinivas, D. & Ratnasamy, P. 2000*b* The structural basis for the enhanced oxygenase activity of copper acetate dimers encapsulated in zeolites. *Topics Catal.* **11/12**, 359–367.

Chavan, S. A., Srinvas, D. & Ratnasamy, P. 2001 Selective oxidation of *para*-xylene to terephthalic acid by μ_3-oxo-bridged Co/Mn cluster complexes encapsulated in zeolite-Y. *J. Catal.* **204**, 409–419.

De Meester, P., Fletcher, R. & Skapski, A. C. 1973 Refined crystal structure of tetra-μ-acetato-bisaquodicopper(II) *J. Chem. Soc. Dalton Trans.*, pp. 2575–2578.

Deshpande, S., Srinivas, D. & Ratnasamy, P. 1999 EPR and catalytic investigation of Cu(salen) complexes encapsulated in zeolites. *J. Catal.* **188**, 261–269.

Farinas, E. T., Alcalde, M. & Arnold, F. 2004 Alkene epoxidation catalyzed by cytochrome P450 BM-3 139-3. *Tetrahedron* **60**, 525–528.

Gleeson, D., Sankar, G., Catlow, C. R. A., Thomas, J. M., Spanò, G., Bordiga, S., Zecchina, A. & Lamberti, C. 2000 The architecture of catalytically active centers in titanosilicate (TS-1) and related selective-oxidation catalysts. *Phys. Chem. Chem. Phys.* **2**, 4812–4817.

Jacob, C. R., Varkey, S. P. & Ratnasmy, P. 1998 Selective oxidation over copper and manganese salens encapsulated in zeolites. *Microporous Mesoporous Mater.* **22**, 465–474.

Notari, B. 1996 Microporous crystalline titanium-silicates. *Adv. Catal.* **41**, 253–334.

Raja, R. & Ratnasamy, P. 1995 Activation of dioxygen by copper complexes incorporated in molecular sieves. *J. Mol. Catal. A* **100**, 93–102.

Raja, R. & Ratnasamy, P. 1997 Direct conversion of methane to methanol. *Appl. Catal. A* **158**, L7–L15.

Raja, R. & Ratnasamy, P. 1997 Selective oxidation of aromatic hydrocarbons over copper complexes encapsulated in molecular sieves. *Stud. Surf. Sci. Catal. B* **105**, 1037–1044.

Raja, R., Jacob, C. R. & Ratnasamy, P. 1999 Direct oxidation of propane to isopropanol. *Catal. Today* **49**, 171–175.

Ratnasmy, P., Srinivas, D. & Knözinger, H. 2004 Active sites and reactive intermediates in titanium silicate molecular sieves. *Adv. Catal.* **48**, 1–169.

Ray, S. & Vasudevan, S. 2003 Encapsulation of cobalt phthalocyanine in zeolite-Y: evidence for nonplanar geometry. *Inorg. Chem.* **42**, 1711–1719.

Seelan, S., Sinha, A. K., Srinivas, D. & Sivasanker, S. 2000 Spectroscopic investigation and catalytic activity of copper (II) phthalocyanine encapsulated in zeolite-Y. *J. Mol. Catal. A* **157**, 163–171.

Shetti, V. N., Manikandan, P., Srinivas, D. & Ratnasamy, P. 2003 Reactive oxygen species in epoxidation reactions over titanosilicate molecular sieves. *J. Catal.* **216**, 461–467.

Shetti, V. N., Srinivas, D. & Ratnasamy, P. 2004 Enhancement of chemoselectivity in epoxidation reactions over TS-1 catalysts by alkali and alkaline metal ions. *J. Mol. Catal. A* **210**, 171–178.

Srinivas, D., Manikandan, P., Laha, S. C., Kumar, R. & Ratnasamy, P. 2003 Reactive oxygen species in epoxidation reactions over titanosilicate molecular sieves. *J. Catal.* **217**, 160–171.

Thomas, J. M. & Sankar, G. 2001 The role of synchrotron-based studies in the elucidation and design of active sites in titanium-silicate epoxidation catalysts. *Acc. Chem. Res.* **34**, 571–581.

Thomas, J. M., Raja, R., Sankar, G., Bell, R. G. & Lewis, D. W. 2001 Benign by design. New catalysts for an environmentally conscious age. *Pure Appl. Chem.* **73**, 1087–1101.